

## Effect of Operating Conditions and Interfering Substances on Photochemical Degradation of a Cationic Surfactant

Bijoli Mondal, Asok Adak & Pallab Datta

To cite this article: Bijoli Mondal, Asok Adak & Pallab Datta (2017): Effect of Operating Conditions and Interfering Substances on Photochemical Degradation of a Cationic Surfactant, Environmental Technology, DOI: [10.1080/09593330.2017.1365943](https://doi.org/10.1080/09593330.2017.1365943)

To link to this article: <http://dx.doi.org/10.1080/09593330.2017.1365943>



Accepted author version posted online: 09 Aug 2017.



Submit your article to this journal [↗](#)



View related articles [↗](#)



View Crossmark data [↗](#)

**Publisher:** Taylor & Francis & Informa UK Limited, trading as Taylor & Francis Group

**Journal:** *Environmental Technology*

**DOI:** 10.1080/09593330.2017.1365943



## **Effect of Operating Conditions and Interfering Substances on Photochemical Degradation of a Cationic Surfactant**

Bijoli Mondal<sup>1</sup>, Asok Adak<sup>1</sup> and Pallab Datta<sup>2</sup>

<sup>1</sup>*Department of Civil Engineering, Indian Institute of Engineering Science and Technology, Shibpur, Howrah 711103, India*

<sup>2</sup>*Center for Healthcare Science and Technology, Indian Institute of Engineering Science and Technology, Shibpur, Howrah 711103, India*

Corresponding Author:

Asok Adak

Department of Civil Engineering

Indian Institute of Engineering Science and Technology Shibpur

Howrah – 711103

India

Email: asok@civil.iests.ac.in, asokadak@gmail.com

Tel: +91-33-2668 4561 (extn. 713)

Fax: +91-33-2668 2916

## Acknowledgement

Bijoli Mondal acknowledges the institute scholarship support received from Ministry of Human Resources and Development, Govt. of India.

## Effect of Operating Conditions and Interfering Substances on Photochemical Degradation of a Cationic Surfactant

### Abstract

This work investigates the degradation kinetics of a recalcitrant organic pollutant, cetyltrimethylammonium bromide (CTAB), using direct UV and UV-H<sub>2</sub>O<sub>2</sub> advanced oxidation processes. Direct photolysis at 253.7 nm showed only 55% degradation upto fluence dose of 40.65 J/cm<sup>2</sup> for initial CTAB concentration of 100 mg/L. The apparent fluence-based pseudo-first order rate constant and quantum yield were  $2.29(\pm 0.325) \times 10^{-5}$  cm<sup>2</sup>/mJ and 0.305(±0.043) mol/Einstein respectively. In case of UV-H<sub>2</sub>O<sub>2</sub>, > 99% degradation was observed upto fluence dose of 0.79 J/cm<sup>2</sup>. The rate constant was ~200 times higher compared to direct photolysis, which was due to hydroxyl radical generation in the UV-H<sub>2</sub>O<sub>2</sub> process. The second order hydroxyl radical rate constant for CTAB was found to be  $1.59(\pm 0.18) \times 10^9$  M<sup>-1</sup>s<sup>-1</sup>. The effects of H<sub>2</sub>O<sub>2</sub> dose, initial CTAB concentration and relevant water quality parameters (pH, alkalinity and nitrate concentrations) were studied; all of these influenced the rate constants. CTAB degradation was also examined in municipal wastewater matrix. It is concluded that UV-H<sub>2</sub>O<sub>2</sub> represents an efficient treatment process for CTAB in environmental matrices.

**Keywords:** advanced oxidation; CTAB; kinetics; UV; scavenging effect

## 1. Introduction

Industrialisation and population growth are resulting in increased discharge of recalcitrant pollutants such as surfactants, pharmaceuticals, personal care products, and dyes into wastewater causing significant global environmental and public health problems. Many of them contain refractory organics, which are difficult or impossible to be eliminated using conventional treatment processes. Among them, surfactants or surface active agents, commonly used in industrial and domestic activities for their amphiphilic characteristics such as detergency, foaming, emulsification, dispersion and solubilization effects have emerged as a major environmental concern [1-2].

Despite their usefulness, the persistent presence of surfactants is potentially hazardous to human health, as well as for terrestrial and aquatic ecosystem. Besides the toxic effects of surfactants, their presence in water below toxic levels are also associated with several pathological, physiological, and biochemical problems on aquatic life. For example, in aquatic plants, these are known to cause break-down of chlorophyll–protein complex, damage to cell membrane, delay in metabolism and reduce growth rate resulting in significant cell death [3].

Amongst surfactants, ionic surfactants comprise approximately 75 % of the total volume, in which cationic surfactants form 10% while rest are anionic surfactants. Although the use of cationic surfactants is less compared to anionic surfactants by volume, they are more toxic and therefore require more intensive efforts for treatment [4]. In the present study, degradation of cetyltrimethylammonium bromide (CTAB), a major cationic surfactant with widespread industrial use has been performed.

There are several techniques for removal of different types of surfactant from wastewater like coagulation [5], adsorption [6], reverse osmosis [7], chemical oxidation [8] and various biological methods [9-10]. However, most of these studies have been performed on anionic surfactant and little attention has been paid on cationic surfactants. It is thus imperative that different industrially important cationic surfactants are also studied for their efficient removal from wastewater. Moreover, all of the above treatment methods have certain limitations. For example, the reverse osmosis system is expensive to install and operate. In coagulation process, large amounts of sludge are generated; while adsorption process results in only phase transfer of pollutants, instead of their elimination. The biological processes are economically more attractive solution for removal of organics. However, treating highly concentrated wastewater using biological process is always difficult. Especially, cationic surfactants like CTAB are known to have antimicrobial activities towards microbes of biological treatment facilities. Due to the fact that conventional biological, physical and chemical treatment methods are not very effective in the removal of cationic surfactants, there exists a need to evaluate alternative options. In recent years, advanced oxidation processes (AOPs) has been explored for the removal of toxic and/or refractory pollutants from wastewaters. Furthermore, AOP pre-treatment followed by biological removal of organics has drawn much attention in recent years [11]. AOPs are based on the chemistry of hydroxyl radicals ( $\text{OH}^\bullet$ ), which are non-selective reactive species with ability to oxidize pollutants into mineral end-products, ultimately yielding  $\text{CO}_2$  and inorganic ions.

AOPs generally used to degrade various recalcitrant pollutants include photochemical process [12-14], photocatalytic processes ( $\text{TiO}_2/\text{UV}$ ) [15] and photo-Fenton process [16]. However, the application of most these processes remain limited due to high operational costs. In addition, Fenton process requires lower pH and continuous pH adjustment, while presence of

iron in wastewater also creates problem. In photocatalytic process, uniform UV irradiation is required. Therefore, to overcome limitations of the above processes, in present study, we propose homogeneous UV-H<sub>2</sub>O<sub>2</sub> AOP as a more efficient option to degrade one of the most widely used cationic surfactant, CTAB. Earlier, Adams and Kuzhikannil [17] explored the UV-H<sub>2</sub>O<sub>2</sub> process for the pre-treatment of some other cationic surfactant to enhance their biodegradability. Since then no investigation has been reported on the kinetics of the UV-H<sub>2</sub>O<sub>2</sub> degradation of CTAB and also influence of different operating parameters applicable for field application. Also hydroxyl radical rate constant for CTAB has not been reported yet. Hydroxyl radicals generated during a UV-H<sub>2</sub>O<sub>2</sub> process are highly reactive to organic molecules [18] and hence this process is expected to effectively degrade CTAB to complete mineralization or intermediate products which could then be removed by biological process.

The objective of this study is to evaluate the effectiveness of degradation of the cationic surfactant, CTAB, in wastewater by UV/H<sub>2</sub>O<sub>2</sub> AOP at different field operating conditions. In particular, the specific aims of this study were as follows: (1) to determine fluence-based reaction rate constants for UV and UV/H<sub>2</sub>O<sub>2</sub> degradation of CTAB; (2) to determine the optimum dose of H<sub>2</sub>O<sub>2</sub> for CTAB degradation; (3) to determine the second order hydroxyl radical rate constant with CTAB; (4) to identify the effects of initial CTAB concentration and (5) to examine the effects of water quality parameters, namely pH, alkalinity, nitrate concentration, and wastewater matrix on CTAB degradation. The goal of the work is to degrade concentrated surfactant solutions generated from industrial sources or from waste streams emanating from adsorption, coagulation-flocculation, and/or reverse osmosis treatment systems to a point where biological processes can treat the transformation products.

## 2. Materials and Methods

### 2.1. Materials

Orange II, and cetyltrimethyloniumbromide (CTAB) were obtained from (Hi-Media, India), while chloroform, 30% H<sub>2</sub>O<sub>2</sub>, sodium phosphate, disodium hydrogen phosphate, and sodium dihydrogen phosphate were all obtained from (Merck, Germany) for use in these experiments. All other chemicals used in this study were of high purity and used without further purification. The strength of the hydrogen peroxide (H<sub>2</sub>O<sub>2</sub>) stock solution was determined by titration method using potassium permanganate.

### 2.2. UV reactor

Direct photolysis and AOP experiments were conducted using batch UV reactor (M/s. Lab Tree, India) system that emits monochromatic light at 253.7 nm. The photograph of the UV reactor is shown in Figure S1. The reactor comprises of eight UV tubes, fitted in a heavy metal enclosure with a highly polished stainless steel reflector. The UV photon flux was measured and monitored throughout the experiments by using potassium ferrioxalate actinometry [19]. The photon flux and fluence of the UV reactor was  $1.9(\pm 0.1) \times 10^{-4}$  Einstein/L-min and  $113(\pm 5.7)$  mJ/cm<sup>2</sup>-min, respectively.

### 2.3. Analytical methods

For determination of cationic surfactant, a simple, cost effective, rapid and reliable ion-pairing indirect spectrophotometric method was employed [20]. Orange II, chemically known as p-( $\beta$ -naphthol-azo) benzene sulfonic acid, having a colour as well as a peak value of wavelength in

spectrophotometric measurement was used as an ion-pairing agent with cationic surfactant. Sample solution (4 ml) containing CTAB in the range of 2 to 12 mg/L was transferred into a 25-mL separating funnel. Then, 1 mL Orange II ( $0.4 \times 10^{-3}$  M) was added followed by addition of 5 mL of chloroform by shaking for 1 min. The aqueous layer was then discarded and the chloroform layer was used for absorbance measurement at a wavelength of 485 nm. This method is free from interfering substances and wide pH variations [20] and has been reported for determination of biodegradation efficiency of cationic surfactants [21].

#### **2.4. UV irradiation and advanced oxidation of cationic surfactants**

Direct photolysis and advanced oxidation experiments were conducted using the batch UV reactor described above. All experiments were conducted using 100 mL of cationic surfactant bearing wastewater and 10 mM phosphate buffer at  $27(\pm 2)$  °C. The samples for direct photolysis were kept in a quartz beaker with upper and lower surfaces covered and irradiated for 6 h. Samples were taken at 30 min intervals and analysed for remaining CTAB concentration. The integrated mass balance for CTAB degradation for first order reaction in the batch reactor can be represented by the following equation [22].

$$\ln \frac{[CTAB]}{[CTAB]_0} = -k'_{app} H' \quad \text{Equation 1}$$

In the above equation, [CTAB] is CTAB concentration at any time t; [CTAB]<sub>0</sub> is initial CTAB concentration;  $k'_{app}$  is apparent fluence based pseudo-first order reaction rate constant ( $\text{cm}^2/\text{mJ}$ ) and  $H'$  is the fluence corresponding to time t ( $\text{mJ}/\text{cm}^2$ ). The apparent fluence-based pseudo-first order rate constant describes transformation of CTAB as a function of UV dose and is thus universally applicable regardless of water quality. For the UV- $\text{H}_2\text{O}_2$  AOP, different peroxide



doses were investigated to identify the maximum degradation kinetics. The following hydrogen peroxide doses were set as the molar ratio of applied  $\text{H}_2\text{O}_2$  to initial CTAB concentration: 0.125, 0.25, 0.5, 1, 2, 5, 7.5, and 10. The pH of the solutions was kept at  $7 \pm 0.1$  using 10 mM phosphate buffer. Samples were taken at regular intervals from 0 to 10 min of irradiation. The experimental results were analysed by above kinetic model (Equation 1). A control experiment was conducted in the dark with 2 mol  $\text{H}_2\text{O}_2$ /mol of CTAB for a period of 30 days. No significant degradation of CTAB was observed during this period. Determination of steady state hydroxyl radical concentration was carried out using para chlorobenzoic acid (pCBA) as a probe compound under similar experimental conditions. Furthermore, the effects of initial concentration of CTAB in the range of 100 - 1000 mg/L were studied.

A competition kinetic study was performed to determine the second order hydroxyl radical rate constant with CTAB. Para chlorobenzoic acid (pCBA) was used as a probe compound for this experiment. The apparent fluence based pseudo-first order rate constant for UV irradiation of pCBA was determined to be  $8 \times 10^{-05} \text{ cm}^2/\text{mJ}$ . The second order rate constant for degradation of pCBA by hydroxyl radical is reported to be  $5.8 \times 10^9 \text{ M}^{-1}\text{s}^{-1}$  [23]. The competition kinetic study was conducted taking both CTAB and pCBA in the same solution in the ratio of 1 mol pCBA per mol CTAB with peroxide dose of 2 mol  $\text{H}_2\text{O}_2$ /mol of CTAB. Samples were collected from the same solution containing both the compounds in the reactor and analysed for both CTAB and pCBA at the same pre-determined time intervals.

The effects of pH (7-12) and other interfering substances (bicarbonate and nitrate) on CTAB degradation were studied. In addition, CTAB degradation experiments were conducted in the municipal wastewater. In all cases, the CTAB concentration was 100 mg/L and suitable

peroxide dose was used. Raw wastewater was collected from municipal sewer having five-day biochemical oxygen demand (BOD<sub>5</sub>) of 200 mg/L, chemical oxygen demand (COD) of 848 mg/L, nitrate of 15 mg/L, total solids of 1334 mg/L, fixed solids of 950 mg/L and dissolved solids of 384 mg/L. The CS concentration in raw wastewater was found to be 3.43(±0.05) mg/L (as CTAB). It was filtered using a commercial filter paper and followed by Whatman 42 filter paper. The filtrate was used to prepare 100 mg/L of CTAB spiked sample.

The biodegradability of intermediate products was examined for transformation of CTAB by UV-H<sub>2</sub>O<sub>2</sub> treatment. The BOD<sub>5</sub> and COD of the degraded samples were measured, and the BOD<sub>5</sub>/COD ratio was used to describe changes in biodegradability.

Results presented here are the mean ± SD for N = 3 unless otherwise stated. Analysis of variance (ANOVA) of the experimental data were carried out in Origin Pro8 software and significant difference was asserted at 95% confidence intervals ( $p < 0.05$ ).

### 3. Results and discussion

#### 3.1. Direct photolysis of CTAB

The degradation of CTAB was studied under UV 253.7 nm for initial CTAB concentration of 100 mg/L. The pH of the solution was 7.1. This degradation study was performed for 6 h. Figure 1 shows that only 55 % degradation of CTAB was achieved in 6 h. The degradation of CTAB followed the pseudo-first order kinetic model. The comparison between first order and second order kinetic models is presented in Supplementary Information. The apparent time-based rate constant was  $2.61 \times 10^{-3} \text{ min}^{-1}$  and the apparent fluence based rate constant was found to be  $2.29 (\pm 0.325) \times 10^{-5} \text{ cm}^2/\text{mJ}$  respectively. For UV based degradation processes, it is difficult to

determine the true rate constant because intermediate products may also absorb light and undergo degradation. Therefore, the determination of apparent rate constant serves the meaningful purpose for field applications and is preferred in literature for understanding and optimizing such processes [22, 24]. Moreover, the UV absorbance at 254 nm of CTAB solution (100 mg/L) and its degraded samples was very low ( $<0.010 \text{ cm}^{-1}$ ) and at 485 nm no absorbance was observed (Figure S2). There was no significant difference ( $p>0.05$ ) in UV absorbance at 254 nm of initial CTAB solution and treated solution at various time. Thus, the degradation of CTAB under direct UV was found to be slow.

[Figure 1 near here]

In addition to determination of rate constant, quantum yields were also calculated for the degradation of CTAB by UV irradiation. The quantum yield is useful for determination of the photolytic efficiency and is defined as the moles of a compound transformed per mole of photons absorbed by the compound [25]. The apparent fluence-based pseudo-first order rate constant was used to calculate the apparent quantum yield (Eq. 2).

$$k'_{p,\text{app}} = \frac{\Phi_{253.7,\text{app}} \varepsilon_{253.7,\text{app}} \ln 10}{U_{253.7}} \quad \text{Equation 2}$$

In Eq. 2,  $k'_{p,\text{app}}$  is the experimentally determined apparent fluence-based pseudo-first order photolysis rate constant ( $\text{cm}^2 \text{ mJ}^{-1}$ ),  $\Phi_{253.7,\text{app}}$  is the apparent quantum yield at 253.7 nm ( $\text{mol Einstein}^{-1}$ ),  $\varepsilon_{253.7,\text{app}}$  is the apparent molar absorptivity at 253.7 nm ( $\text{M}^{-1} \text{ cm}^{-1}$ ), and  $U_{253.7}$  is the molar photon energy at 253.7 nm ( $4.72 \times 10^5 \text{ J Einstein}^{-1}$ ). The apparent quantum yield for degradation of CTAB was found to be  $0.305 (\pm 0.043) \text{ mol Einstein}^{-1}$ . Comparable quantum

yields of 0.582 mol Einstein<sup>-1</sup> and 1.344 mol Einstein<sup>-1</sup> for CTAB and linear alkylbenzenesulfonate (LAS) were reported as respectively in previous studies [26-27].

### 3.2. Advanced oxidation process of CTAB by UV-H<sub>2</sub>O<sub>2</sub> process

According to the above results, it can be inferred the UV radiation did not achieve rapid CTAB degradation. It may be expected that UV based AOP i.e. UV-H<sub>2</sub>O<sub>2</sub> can improve the efficiency of degradation. Figure 2 shows the CTAB degradation efficiency in presence of H<sub>2</sub>O<sub>2</sub> at molar ratios of 2 (mol of H<sub>2</sub>O<sub>2</sub> / mol of CTAB) at pH 7. The initial concentration of CTAB was 100 mg/L. It was noticed that almost 100 % degradation of CTAB was achieved within 7 min. These results indicate that the hydroxyl radical yield from UV-H<sub>2</sub>O<sub>2</sub> process (i.e. 1 mol/1 mol H<sub>2</sub>O<sub>2</sub>) was the driving force behind enhanced degradation of CTAB. The contribution of hydroxyl radicals to the total degradation of CTAB was found to be almost 100%. Hydroxyl radical oxidizes the surfactant molecules (R-H) by hydrogen abstraction generating organic radicals (R<sup>•</sup>). Then these organic radicals undergo oxidative chain reactions leading to form various by-products [28]. Kinetic analysis showed that the degradation followed the pseudo-first order kinetic model. The apparent time-based rate constant and fluence based rate constant were found to be 0.5003(±0.1) min<sup>-1</sup> and 4.43(±0.88)×10<sup>-3</sup> cm<sup>2</sup>/mJ respectively. The rate constants found in this case were ~200 times higher compared to CTAB degradation through direct UV.

[Figure 2 near here]

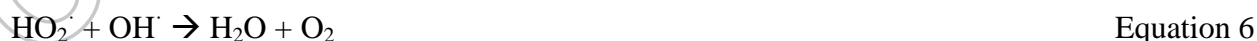
At a disinfection-level UV dose of 40-190 mJ/cm<sup>2</sup>, negligible (< 0.25%) direct UV degradation is expected for CTAB. However, the same fluence with a ratio of 2 mol H<sub>2</sub>O<sub>2</sub>/mol CTAB yields transformation efficiencies of 5% and 24% for 40 and 190 mJ/cm<sup>2</sup> respectively.

UV doses typically employed in advanced oxidation are 540–2000 mJ/cm<sup>2</sup> [29-30]. Increasing the fluence to 790 mJ/cm<sup>2</sup> and employing 2 mol H<sub>2</sub>O<sub>2</sub>/mol CTAB allowed almost 100% degradation of CTAB.

### 3.3. Effect of H<sub>2</sub>O<sub>2</sub> dose

The UV/H<sub>2</sub>O<sub>2</sub> process is a photochemical process, the cost of both energy and oxidant (H<sub>2</sub>O<sub>2</sub>) should be considered and it is necessary to determine the optimum dose of H<sub>2</sub>O<sub>2</sub> for the process.

Experiments were conducted by varying peroxide doses with initial CTAB concentration of 100 mg/L, keeping the pH constant at 7. From figure 3, it is noticed that the pseudo-first order rate constant for CTAB degradation increased upto a H<sub>2</sub>O<sub>2</sub> dose of 1 mol H<sub>2</sub>O<sub>2</sub>/ mol CTAB. Above 1 mol H<sub>2</sub>O<sub>2</sub>/mol CTAB, no significant difference ( $p > 0.05$ ) in the rate constant was observed between the groups 1 to 5 mol H<sub>2</sub>O<sub>2</sub>/mol CTAB. At higher peroxide dose, additional H<sub>2</sub>O<sub>2</sub> did not increase appreciably the degradation efficiency. This may be due to hydroxyl radicals reacting with excess H<sub>2</sub>O<sub>2</sub> rather than CTAB molecules [22, 31]. Excess of H<sub>2</sub>O<sub>2</sub> results in competition reaction with hydroxyl radical as given below [32].



From the above equations, it is understood that the hydroxyl radical is consumed by the excess of H<sub>2</sub>O<sub>2</sub>. Furthermore, the steady state hydroxyl radical concentrations under the experimental

conditions were determined to be  $1.58(\pm 0.18) \times 10^{-12}$ ,  $2.33(\pm 0.27) \times 10^{-12}$ ,  $2.71(\pm 0.31) \times 10^{-12}$ ,  $4.97(\pm 0.57) \times 10^{-12}$ ,  $5.18(\pm 0.44) \times 10^{-12}$ ,  $4.87(\pm 0.55) \times 10^{-12}$ ,  $4.50(\pm 0.51) \times 10^{-12}$  and  $4.18(\pm 0.48) \times 10^{-12}$  M at 0.125, 0.25, 0.5, 1.0, 2.0, 3.0, 4.0 and 5.0 mol  $\text{H}_2\text{O}_2$ /mol CTAB respectively. The hydroxyl radical concentration was found to increase sharply upto a  $\text{H}_2\text{O}_2$  dose of 1 mol  $\text{H}_2\text{O}_2$ /mol CTAB; beyond 1 mol  $\text{H}_2\text{O}_2$ /mol CTAB, there was no significant ( $p > 0.05$ ) change in its concentration. Therefore, the optimum concentration of  $\text{H}_2\text{O}_2$  can be considered to be 1 mol  $\text{H}_2\text{O}_2$ /mol CTAB. The fraction of hydroxyl radical reacting with CTAB at 0.125, 0.25, 0.5, 1.0, 2.0, 3.0, 4.0 and 5.0 mol  $\text{H}_2\text{O}_2$ /mol CTAB was 0.883, 0.915, 0.936, 0.958, 0.961, 0.96, 0.957 and 0.952 respectively.

[Figure 3 near here]

### **3.4. Effect of initial CTAB concentration**

The degradation of CTAB was studied at different initial concentrations (100 - 1000 mg/L) with  $\text{H}_2\text{O}_2$  dose of 2 mol  $\text{H}_2\text{O}_2$ /mol CTAB and at a pH of 7. It was observed that with increase in CTAB concentration, the percentage degradation of CTAB gradually decreased (Figure 4). The degradation of CTAB was found to be almost 100% at an initial CTAB concentration of 100 mg/L; while, the degradation was found to be 55, 26 and 15% for initial CTAB concentration of 200, 500 and 1000 mg/L respectively; which were significantly different from each other ( $p < 0.05$ ). Similar behaviour has been observed in degradation of compounds like microcystin – LR and Diethanolamine (DEA), using the UV/ $\text{H}_2\text{O}_2$  process [33-34]. The molar absorptivity of CTAB and  $\text{H}_2\text{O}_2$  are  $14.6$  and  $19.6 \text{ M}^{-1}\text{cm}^{-1}$  respectively. Thus, it is expected that the production of hydroxyl radical will not be affected at higher CTAB concentration. However, when CTAB

concentration is high, the concentration of H<sub>2</sub>O<sub>2</sub> is also high which may scavenge the hydroxyl radical. Thus, the rate constant decreased with the increasing CTAB concentration.

[Figure 4 near here]

### **3.5. Competition kinetic study for determining second order hydroxyl radical rate constants with CTAB**

Competition kinetic experiments were conducted to determine the second order rate constant of reaction between hydroxyl radical with CTAB. Here, pCBA was used as a hydroxyl radical probe compound [22]. In the absence of H<sub>2</sub>O<sub>2</sub>, surfactant and pCBA showed fractional degradation by UV light at 253.7 nm. The corresponding pseudo-first order rate constants for UV irradiation were included in the competition kinetics relationship. The integrated form of the mass balance on CTAB in the batch reactor can be written as shown in Eq. (7).

$$-\ln \frac{[\text{CTAB}]}{[\text{CTAB}]_0} = k'_{p, \text{CTAB}} H' + k''_{\text{OH}\cdot, \text{CTAB}} \int_0^t [\text{OH}\cdot] dt \quad \text{Equation 7}$$

In Eq. (7), [CTAB] is the concentration of CTAB at time t,  $k'_{p, \text{CTAB}}$  is the apparent fluence-based pseudo-first order rate constant for CTAB, [OH·] is the hydroxyl radical concentration, and  $k''_{\text{OH}\cdot, \text{CTAB}}$  is the second order rate constant for degradation of CTAB by hydroxyl radicals. Degradation of a pCBA can be described by a similar relationship (Eq. (8)).

$$-\ln \frac{[\text{pCBA}]}{[\text{pCBA}]_0} = k'_{p, \text{pCBA}} H' + k''_{\text{OH}\cdot, \text{pCBA}} \int_0^t [\text{OH}\cdot] dt \quad \text{Equation 8}$$

Since pCBA and CTAB were irradiated simultaneously in same solution, we assume that pCBA and surfactant experience the same hydroxyl radical exposure (i.e.,  $\int_0^t [HO \cdot] dt$ ). Therefore, Eq. 7 and 8 can be combined together to give Eq. (9) which can be used to determine  $k''_{OH,CTAB}$ .

$$\ln \frac{[CTAB]}{[CTAB]_0} + k'_{p,CTAB} H' = \left[ \ln \frac{[pCBA]}{[pCBA]_0} + k'_{p,pCBA} H' \right] \frac{k''_{OH,CTAB}}{k''_{OH,pCBA}} \quad \text{Equation 9}$$

Therefore, from the slope of a plot of  $\ln \frac{[CTAB]}{[CTAB]_0} + k'_{p,CTAB} H'$  vs

$\left[ \ln \frac{[pCBA]}{[pCBA]_0} + k'_{p,pCBA} H' \right] \frac{1}{k''_{OH,pCBA}}$ ;  $k''_{OH,CTAB}$  can be directly determined as noted in Figure 5.

The second order hydroxyl radical rate constants with CTAB was found to be  $1.59(\pm 0.18) \times 10^9 \text{ M}^{-1} \text{ s}^{-1}$ . The second order hydroxyl radical rate constants with sodium dodecylbenzenesulfonate and lauryl sulfate have been reported as  $1.6(\pm 0.1) \times 10^{10}$  and  $8.2 \times 10^9 \text{ M}^{-1} \text{ s}^{-1}$  respectively [35-36].

[Figure 5 near here]

### 3.6. Effect of pH

The wastewater generated from textiles and other industries using surfactants is generally alkaline in nature. Thus the effect of pH in the range of 7-12 on UV-H<sub>2</sub>O<sub>2</sub> degradation of CTAB was studied. The experiments were conducted with initial CTAB concentration of 100 mg/L and a peroxide dose of 1 mol H<sub>2</sub>O<sub>2</sub>/mol CTAB. It was noticed that the first order rate constants were not significantly different ( $p > 0.05$ ) in the pH range of 7-10 (Figure 6). Further increase in pH beyond 10 resulted in significant ( $p < 0.05$ ) decrease in rate constant. Interestingly, the removal efficiency was not changed significantly. Similar observation has been reported for degradation



of other textile surfactants by UV-H<sub>2</sub>O<sub>2</sub> process [37]. The decrease in rate constant at pH 11 and 12 might be due to dissociation of H<sub>2</sub>O<sub>2</sub> at higher pH. Being a weak acid (pK<sub>a</sub> =11.8), H<sub>2</sub>O<sub>2</sub> dissociates to hydroperoxide (HO<sub>2</sub><sup>-</sup>) anion as shown below.



The HO<sub>2</sub><sup>-</sup> is dominant at pH > 10 [35]. The HO<sub>2</sub><sup>-</sup>, conjugate anions of H<sub>2</sub>O<sub>2</sub> reacts with undissociated H<sub>2</sub>O<sub>2</sub> and hydroxyl radical [38].



Thus, the steady state concentration of hydroxyl radical is lowered than expected. The steady state concentration of hydroxyl radical was determined to be 4.93(±0.56)×10<sup>-12</sup>, 5.45(±0.62)×10<sup>-12</sup>, 5.48(±0.62)×10<sup>-12</sup>, 5.09(±0.58)×10<sup>-12</sup>, 3.93(±0.45)×10<sup>-12</sup> and 3.87(±0.26)×10<sup>-12</sup> M for pH 7, 8, 9, 10, 11 and 12 respectively. Also, the reactivity of O<sub>2</sub><sup>· -</sup> with organic pollutants is very low [39]. Therefore, it is concluded that if the wastewater is having pH more than 11, it should be adjusted to 7 - 10 for faster degradation before treatment.

[Figure 6 near here]

### 3.7. Effect of bicarbonate

The effect of bicarbonate concentration on CTAB degradation (0-10 mM) was investigated for solutions containing 100 mg/L of CTAB with a peroxide dose of 2 mol H<sub>2</sub>O<sub>2</sub>/mol CTAB at pH of 7. The second order rate constant for reaction of bicarbonate with hydroxyl radicals was

reported to be  $8.5 \times 10^6 \text{ M}^{-1} \text{ s}^{-1}$  [23]. This reaction rate is much slower than hydroxyl radical reaction with CTAB, for which a rate constant of  $1.59 \times 10^9 \text{ M}^{-1} \text{ s}^{-1}$  was determined. The apparent fluence-based rate constant decreased significantly with the addition of bicarbonate as shown in Figure 7. The fraction of hydroxyl radicals that reacts with bicarbonate compared to all other species is expressed by Eq. 13 (adapted from [22]).

$$f_{\text{HO}\cdot, \text{HCO}_3^-} = \frac{k''_{\text{HO}\cdot, \text{HCO}_3^-} [\text{HCO}_3^-]}{k''_{\text{HO}\cdot, \text{CTAB}} [\text{CTAB}] + k''_{\text{HO}\cdot, \text{HCO}_3^-} [\text{HCO}_3^-] + \sum_{i=1}^n k''_{\text{HO}\cdot, \text{S}_i} [\text{S}_i]}$$

Equation 13

Where,  $[\text{S}_i]$  is the concentration of other hydroxyl radical scavengers like carbonate, phosphate, and hydrogen peroxide;  $k''_{\text{HO}\cdot, \text{S}_i}$  is the second order rate constant for reaction of scavengers with hydroxyl radicals;  $k''_{\text{HO}\cdot, \text{HCO}_3^-}$  the second order rate constant for degradation of carbonate by hydroxyl radicals and  $k''_{\text{HO}\cdot, \text{CTAB}}$  the second order rate constant for degradation of CTAB by hydroxyl radicals. The fraction of hydroxyl radicals consumed by bicarbonate was calculated to be  $18.5 \times 10^{-3}$ ,  $44.9 \times 10^{-3}$ ,  $85.9 \times 10^{-3}$ , and  $158.3 \times 10^{-3}$  for bicarbonate concentrations of 1, 2.5, 5, and 10 mM, respectively. Hydroxyl radical scavenging by bicarbonate resulted in a lower fraction of hydroxyl radicals reacting with CTAB (*i.e.*,  $f_{\text{HO}\cdot, \text{CTAB}} = 0.94, 0.92, 0.88$  and  $0.81$ ) respectively. The hydroxyl radical demand of hydrogen peroxide and phosphate was about 3.2% and 0.22% respectively. These findings indicate that alkalinity differences in surfactant contaminated water will impact the observed reaction kinetics in UV- $\text{H}_2\text{O}_2$  systems; furthermore, these findings also suggest that real water matrices containing high concentrations of dissolved organic matter may further determine surfactant treatment efficiency through hydroxyl radical scavenging.

[Figure 7 near here]

### 3.8. Effect of nitrate concentration

Generally, surface water and wastewater contain high concentrations of nitrate. The effect of nitrate (0-1 mM) on CTAB photodegradation was studied. In these experiments, initial CTAB concentration was taken as 100 mg/L. The peroxide dose and pH were 2 mol H<sub>2</sub>O<sub>2</sub>/mol for CTAB and 7 respectively. Experimental data were analyzed using a first order kinetic model and apparent fluence-based pseudo-first order rate constants were calculated (Figure 8). The observed rate constant decreased linearly for nitrate concentrations of 0 to 1 mM (with significant difference between each nitrate concentration group tested,  $p < 0.05$ ) due to scavenging of hydroxyl radicals by nitrate ( $k''_{\text{HO}\cdot, \text{NO}_3^-} = 9.7 \times 10^9 \text{ M}^{-1} \text{ s}^{-1}$  [23]). The fractions of hydroxyl radicals consumed by nitrate were calculated to be 0.84, 0.91, 0.94 and 0.95 for nitrate concentrations of 0.25, 0.50, 0.75 and 1.0 mM, respectively. Hydroxyl radical scavenging by nitrate, therefore, resulted in a lower fraction of hydroxyl radicals reacting with CTAB (*i.e.*,  $f_{\text{HO}\cdot, \text{CTAB}} = 0.15, 0.08, 0.05, \text{ and } 0.04$  respectively). The hydroxyl radical demand of hydrogen peroxide for these experiments was approximately 3%. The effect of nitrate was found to be more pronounced compared to alkalinity of water sample.

[Figure 8 near here]

### 3.9. Effect of municipal wastewater on surfactant degradation

CTAB solution having initial concentration of 100 mg/L was prepared with filtered municipal wastewater having BOD<sub>5</sub> of 200 mg/L, COD of 848 mg/L, total solids of 1334 mg/L, fixed solids of 950 mg/L and dissolved solids of 384 mg/L. The [H<sub>2</sub>O<sub>2</sub>]/[CTAB] was 2 and the pH was

7.1 ± 0.1. The degradation of CTAB in this case was found to be lesser compared to distilled water spiked samples (Figure 9). For example, the degradation of CTAB at 4 min was found to be 80% and 50% for distilled water spiked and wastewater spiked samples respectively. The fluence based rate constant for this case was found to be 2.20×10<sup>-3</sup> cm<sup>2</sup>/mJ and the time-based rate constant for this case was found to be 0.2522 min<sup>-1</sup> which was found to be 2-times lower compared to the rate constant found in case of distilled water spiked samples at pH 7. The decrease in rate constant for wastewater may be due to either shading effect caused by the high UV absorbance of wastewater (UV<sub>254</sub> = 0.508 cm<sup>-1</sup>) or scavenging of hydroxyl radicals by dissolved organic matter (DOM) and other wastewater matrices. In order to determine the more significant cause of the reduction in rate constant, we calculated the theoretical and observed light screening factors as given below [40].

$$S_{th} = \frac{1 - e^{-2.3Al}}{2.30 Al} \quad \text{Equation 14}$$

$$S_{obs} = \frac{k'_{WW}}{k'_{DW}} \quad \text{Equation 15}$$

In the above equations,  $S_{th}$  is the theoretical light screening factor;  $S_{obs}$  is the observed light screening factor;  $A$  is the absorbance of sample;  $l$  is the path length (cm);  $k'_{WW}$  is rate constant of CTAB degradation in wastewater matrix and  $k'_{DW}$  is rate constant of CTAB degradation in distilled water. The theoretical and observed light screening factors were found to be 0.59 and 0.5 respectively. As the ratio of observed and theoretical light screening factor is less than 1, it can be concluded that hydroxyl radical scavenging by wastewater matrix is significant compared to light shading effect for causing the reduction in degradation [41]. These results are in consonance with other documented results [41-42].

[Figure 9 near here]

### **3.10. Biodegradability enhancement after UV-H<sub>2</sub>O<sub>2</sub> treatment**

Due to the high operating costs of AOPs for complete mineralization of organics application of short-term AOPs followed by biological treatment is being pursued for recalcitrant pollutants like CTAB [41]. Therefore, we measured the biodegradability of the UV-H<sub>2</sub>O<sub>2</sub> treated wastewater containing CTAB. In particular, 100 mg/L CTAB solutions were treated by UV-H<sub>2</sub>O<sub>2</sub> for 2, 4, 6, 8 and 10 min. The H<sub>2</sub>O<sub>2</sub> dose was 2 mol H<sub>2</sub>O<sub>2</sub> per mol of CTAB. Residual H<sub>2</sub>O<sub>2</sub> in the treated samples was quenched by catalase before measurement of COD and BOD<sub>5</sub>. The initial BOD<sub>5</sub>/COD ratio for 100 mg/L of CTAB solution was found to be 0.11 ( $\pm 0.02$ ), indicating that CTAB is not biodegradable [43]. On the other hand, the BOD<sub>5</sub>/COD ratio increased from 0.11 to 0.67 within 10 min of UV-H<sub>2</sub>O<sub>2</sub> treatment (Figure 10). It was noticed that the increase in BOD<sub>5</sub>/COD was sharp from 0 - 6 min; however, there was insignificant change ( $p > 0.05$ ) in BOD<sub>5</sub>/COD for the treatment time range 6 - 10 min. The BOD<sub>5</sub> value increased from 22 to 62 mg/L in first 6 min. These results demonstrate that the transformation products were more biodegradable than the CTAB parent compound. Since the BOD<sub>5</sub>/COD ratio in UV-H<sub>2</sub>O<sub>2</sub> effluent was 0.67, the effluent can be effectively treated by biological processes.

[Figure 10 near here]

## **4. Conclusions**

In summary, disinfection-level UV treatment at 253.7 nm transforms a nominal fraction of CTAB in water and indicates the need for higher fluence to attain significant degradation efficiencies. For the UV-H<sub>2</sub>O<sub>2</sub> process, more than 99% degradation of CTAB was achieved with

a fluence of 790 mJ/cm<sup>2</sup> and peroxide dose of 2 mol H<sub>2</sub>O<sub>2</sub>/mol CTAB. The rate constants for UV irradiation at 253.7 nm and degradation by hydroxyl radicals are comparable to other systems; however, pH, alkalinity and nitrate concentrations may affect surfactant degradation. The pH in the range of 10-12 demonstrated significant effect on CTAB degradation. The degradation of CTAB was adversely affected with the increase in nitrate concentration in the range of 0 to 1 mM. The addition of bicarbonate demonstrated significant decrease in the CTAB degradation rate constant compared to no alkalinity condition. The second order hydroxyl radical rate constant for CTAB was found to be  $1.59(\pm 0.18) \times 10^9 \text{ M}^{-1} \text{ s}^{-1}$ . Municipal wastewater matrix showed adverse effect on CTAB degradation compared to distilled water spiked samples. The UV-H<sub>2</sub>O<sub>2</sub> process provides quick and efficient transformation of CTAB to biodegradable products that can be more successfully treated via conventional biological processes. Therefore, the UV-H<sub>2</sub>O<sub>2</sub> process is proposed for treatment of concentrated surfactant solutions generated from industrial sources or from waste streams emanating from adsorption, coagulation-flocculation, and/or reverse osmosis treatment systems.

### Supplementary Information

The photograph of the batch UV reactor is presented in supplementary Information.

### 5. Reference

- [1] Koner S, Pal A, Adak A. Utilization of silica gel waste for adsorption of cationic surfactant and adsolubilization of organics from textile wastewater: A case study. *Desalination*. 2011;276:142–147.
- [2] Rivera-Utrilla J, Bautista-Toledo MI, Sanchez-Polo M, et al. Removal of surfactant

dodecylbenzenesulfonate by consecutive use of ozonation and biodegradation. Eng. Life Sci. 2012;12(1):113–116.

- [3] Onder E, Koparal AS, Ogutveren UB. An alternative method for the removal of surfactants from water: Electrochemical coagulation. Sep. Purif, 2007;52:527–532.
- [4] Chebotarev AN, Paladenko TV, Shcherbakova TM. Adsorption – photometric determination of cationic surfactant traces. J. Anal. Chem. 2004; 59(4):349–353.
- [5] Bobirica C, Dabija G, Bobirica L, et al. Performance evaluation of anionic polymer-cationic surfactant complex coagulants in water treatment. Environ. Engg. Manag. J. 2014; 13(8):2045–2050.
- [6] Kyzas GZ, Peleka EN, Deliyanni EA. Nanocrystalline akaganeite as adsorbent for surfactant removal from aqueous solutions. Materials. 2013;6:184–197.
- [7] Kowalska I. Separation of anionic surfactants in a sequential ultrafiltration – ion exchange purification system. J. Environ. Stud. 2012;21 (3):677–684.
- [8] Lin SH, Lin CM, Leu HG. Operating characteristics and kinetic studies of surfactant wastewater treatment by Fenton oxidation. Wat. Res. 1999;33(7):1735–1741.
- [9] Hossain M, Mondal IH. Biodegradable surfactant from natural starch for the reduction of environmental pollution and safety for water living organism. Int. J. Innov. Res. Adv. Eng. 2014;1(8):424–433.
- [10] Othman MZ, Ding L, Jiao Y. Effect of anionic and non-ionic surfactants on activated sludge

oxygen uptake rate and nitrification. World Acad. Sci. Eng. Technol. 2009;3(10):1147–1153.

[11] Rodrigues CSD, Madeira LM, Boaventura RAR. Synthetic textile dyeing wastewater treatment by integration of advanced oxidation and biological processes - Performance analysis with costs reduction. J. Environ. Chem. Eng. 2014;2:1027–1039.

[12] Ghaderpoori M, Dehghani MH. Investigating the removal of linear alkyl benzene sulfonate from aqueous solution by ultraviolet irradiation and hydrogen peroxide process. Desalin. Water Treat. 2015;57(32):15208–15212.

[13] Paphane BD, Ramirez LLZ. Chemical pre-treatment of anionic surfactants contaminated waste water at Enapol A.S. using  $H_2O_2$ /UV light waste water pre-treatment method. Environ. Anal. Toxicol. 2013;3(4):3–6.

[14] Sanz J, Lombraña JJ, Luis A. Temperature-assisted UV/ $H_2O_2$  oxidation of concentrated linear alkylbenzene sulphonate (LAS) solutions. Chem. Eng. J. 2013;215–216:533–541.

[15] Samadi TM, Dorraji SSM, Atashi Z, et al. Photo catalytic removal of sodium dodecyl sulfate from aquatic solutions with prepared ZnO nanocrystals and UV irradiation. Avicenna of J. Env. Heal. Eng. 2014;1(1):217–225.

[16] Chitra S, Paramasivan K, Shanmugamani AG, et al. Advanced oxidation processes for the treatment of surfactant wastes. . Chem. Eng. Chem. Res. 2014;1(3):163–173.

[17] Adams CD, Kuzhikannil JJ. Effects of UV/ $H_2O_2$  preoxidation on the aerobic biodegradability of quaternary amine surfactants. Wat. Res. 2000;34(2):668–672.



- [18] Zepp RG, Faust BC, Hoign J. Hydroxyl radical formation in aqueous reactions (pH 3–8) of iron(II) with hydrogen peroxide: The photo-Fenton reaction. *Environ. Sci. Technol.* 1992;26(2):313–319.
- [19] Hatchard CG., Parker, CAA. new sensitive chemical actinometer. II. potassium ferrioxalate as a standard chemical actinometer, *Proceedings of the Royal Society A.* 1956;235:518–536
- [20] Few AV, Ottewill RHA. Spectrophotometric method for the determination of cationic detergents. *J. Colloid. Sci.* 1956;38:34–38.
- [21] Liu H, Hu Z, Zhou X, et al. Synthesis, corrosion inhibition performance and biodegradability of novel alkyl hydroxyethyl imidazoline salts. *J Surfact Deterg* 2015;18:1025–1031.
- [22] Adak A, Mangalgiri KP, Lee J, et al. UV irradiation and UV-H<sub>2</sub>O<sub>2</sub> advanced oxidation of the roxarsone and nitarosone organoarsenicals. *Wat. Res.* 2015;70:74–85.
- [23] Buxton GV, Greenstock CL, Helman WP, et al. Critical review of rate constants for reactions of hydrated electrons, hydrogen atoms and hydroxyl radicals ( $\cdot\text{OH}/\text{O}$ ) in aqueous solution. *J. Phys. Chem. Ref. Data.* 1988;17(2):513–886.
- [24] Zheng S, Cai Y, O'Shea KE. TiO<sub>2</sub> photocatalytic degradation of phenylarsonic acid. *Journal of Photochemistry and Photobiology A: Chemistry* 2010;210:61–68
- [25] Bolton JR, Stefan MI. Fundamental photochemical approach to the concepts of fluence (UV dose) and electrical energy efficiency in photochemical degradation reactions. *Res. Chem. Intermed.* 2002;28:857–870.

- [26] Acharya S, Rebery B. Fluorescence spectrometric study of eosin yellow dye – surfactant interactions. *Arab. J. Chem.* 2009;2:7–12.
- [27] Sanz J, Lombraña JI, Luis A. Ultraviolet- $\text{H}_2\text{O}_2$  oxidation of surfactants. *Env. Chem Lett.* 2003;1:32–37.
- [28] Chitra S, Paramasivan K, Shanmugamani A., et al. Advanced oxidation processes for the treatment of surfactant wastes. *J Chem Eng Chem Res* 2014;1:163-173.
- [29] Baeza C, Knappe DRU. Transformation kinetics of biochemically active compounds in low-pressure UV Photolysis and UV/ $\text{H}_2\text{O}_2$  advanced oxidation processes. *Wat. Res.*, 2011;45(15):4531–4543.
- [30] Keen OS, Love NG, Linden KG. The role of effluent nitrate in trace organic chemical oxidation during UV disinfection. *Wat. Res.* 2012;46(16):5224–5234.
- [31] Lopez A, Bozzi A, Mascolo G, et al. Kinetic investigation on UV and UV/ $\text{H}_2\text{O}_2$  degradations of pharmaceutical intermediates in aqueous solution. *J. Photochem. Photobiol. A Chem.* 2003;156(1–3):121–126.
- [32] Baxendale JH, Wilson JA. The photolysis of hydrogen peroxide at high intensities. *Transactions of the Faraday Society* 1957;53: 344-356.
- [33] He X, Pelaez M, Westrick JA, et al. Efficient removal of microcystin-LR by UV-C/ $\text{H}_2\text{O}_2$  in synthetic and natural water samples. *Wat. Res.* 2011;46 (5):1501–1510.
- [34] Madihah N, Yaser B, Chemat F, et al. Degradation of aqueous diethanolamine (DEA)

solutions using UV/H<sub>2</sub>O<sub>2</sub> process. Chem. Eng. Trans. 2015;43:1–6.

- [35] Ikehata K, El-din MG. Degradation of recalcitrant surfactants in wastewater by ozonation and advanced oxidation process: a review. Ozone Sci. Eng. 2004;327–343.
- [36] Horváth O, Huszánk R. Degradation of surfactants by hydroxyl radicals photogenerated from hydroxoiron (III) complexes. Photochem. Photobiol. Sci. 2003;2:960–966.
- [37] Alaton IA, Cokgor EU, Koban B. Integrated photochemical and biological treatment of a commercial textile surfactant: process optimization, process kinetics and COD fractionation. J. Hazard. Mater. 2007;146:453–458.
- [38] Ríos F, Kaucharczyk MO, Gmurek M, et al. Removal efficiency of anionic surfactants from water during UVC photolysis and advanced oxidation process in H<sub>2</sub>O<sub>2</sub>/UVC systems. Archives of Environmental Protection. 2017;43(1):20-26.
- [39] Braun AM, Maurette MT, Oliveros E. Photochemical technology. Chichester: Wiley; 1991
- [40] Walse SS, Morgan SL, Kong L, et al. Role of dissolved organic matter, nitrate, and bicarbonate in the photolysis of aqueous fipronil. Environ. Sci. Technol. 2004;38(14):3908-3915.
- [41] Cater SR, Stefan MI, Bolton JR, et al. UV/H<sub>2</sub>O<sub>2</sub> treatment of methyl tert-butyl ether in contaminated waters. Environ. Sci. Technol. 2000;34:659–662.
- [42] Wang GS, Liao CH, Chen HW, et al. Characteristics of natural organic matter degradation in water by UV/H<sub>2</sub>O<sub>2</sub> treatment. Environ. Technol. 2006;27:277–287.

- [43] Lafi WK, Al-Qodah Z. Combined advanced oxidation and biological treatment processes for the removal of pesticides from aqueous solutions. *J. Hazard. Mater.* 2006;137:489–497.

### Figure Captions

Figure 1. Degradation of CTAB (100 mg/L) spiked in distilled water at UV 253.7 nm at pH 7.0 ( $\pm 0.1$ )

Figure 2. Degradation of CTAB (100 mg/L) spiked in distilled water by UV- $\text{H}_2\text{O}_2$  process with  $[\text{H}_2\text{O}_2]/[\text{CTAB}] = 2$  at pH 7.0 ( $\pm 0.1$ )

Figure 3. Effect of  $\text{H}_2\text{O}_2$  dose on apparent fluence-based pseudo-first order rate constant for CTAB (100 mg/L) degradation at pH 7.0 ( $\pm 0.1$ ) ( $p = 0.0002$  for groups  $[\text{H}_2\text{O}_2]/[\text{CTAB}] = 0$  to 1 and  $p = 0.9505$  for groups  $[\text{H}_2\text{O}_2]/[\text{CTAB}] = 1$  to 5)

Figure 4. Effect of initial concentration on CTAB degradation with  $[\text{H}_2\text{O}_2]/[\text{CTAB}] = 2$  at pH 7.0 ( $\pm 0.1$ ) ( $p = 0.0004$  for CTAB concentration range 100 to 1000 mg/L)

Figure 5. Determination of the second order rate constant for CTAB (100 mg/L) transformation by hydroxyl radicals using competition kinetic study at pH 7.0 ( $\pm 0.1$ )

Figure 6. Effect of solution pH on removal efficiency for a fluence of 790 mJ/cm<sup>2</sup> with the corresponding apparent fluence-based pseudo-first order rate constant for CTAB degradation by UV-H<sub>2</sub>O<sub>2</sub> process with [H<sub>2</sub>O<sub>2</sub>]/[CTAB] = 1 ( $p = 0.8119$  for pH range 7 to 10 and  $p = 0.0306$  for pH range 10 to 12)

Figure 7. Effect of alkalinity (expressed as HCO<sub>3</sub><sup>-</sup> concentration) on CTAB (100 mg/L) degradation process with [H<sub>2</sub>O<sub>2</sub>]/[CTAB] = 2 and pH 7.0 ( $\pm 0.1$ ) ( $p = 0.0420$  between 0 and 2.5 mM bicarbonate)

Figure 8. Effect of nitrate on CTAB (100 mg/L) degradation in the UV-H<sub>2</sub>O<sub>2</sub> process with [H<sub>2</sub>O<sub>2</sub>]/[CTAB] = 2 and pH 7.0 ( $\pm 0.1$ ) ( $p = 0.0056$  for 0 to 1 mM nitrate concentration)

Figure 9. Degradation of CTAB spiked in municipal wastewater by UV-H<sub>2</sub>O<sub>2</sub> process with initial CTAB concentration of 100 mg/L, [H<sub>2</sub>O<sub>2</sub>]/[CTAB] = 2 at pH 7.0 ( $\pm 0.1$ )

Figure 10. Effect of UV-H<sub>2</sub>O<sub>2</sub> treatment on biodegradability index of 100 mg/L CTAB ( $p = 1.33 \times 10^{-9}$  for 0 to 6 min and  $p = 0.0715$  for 6 to 10 min)

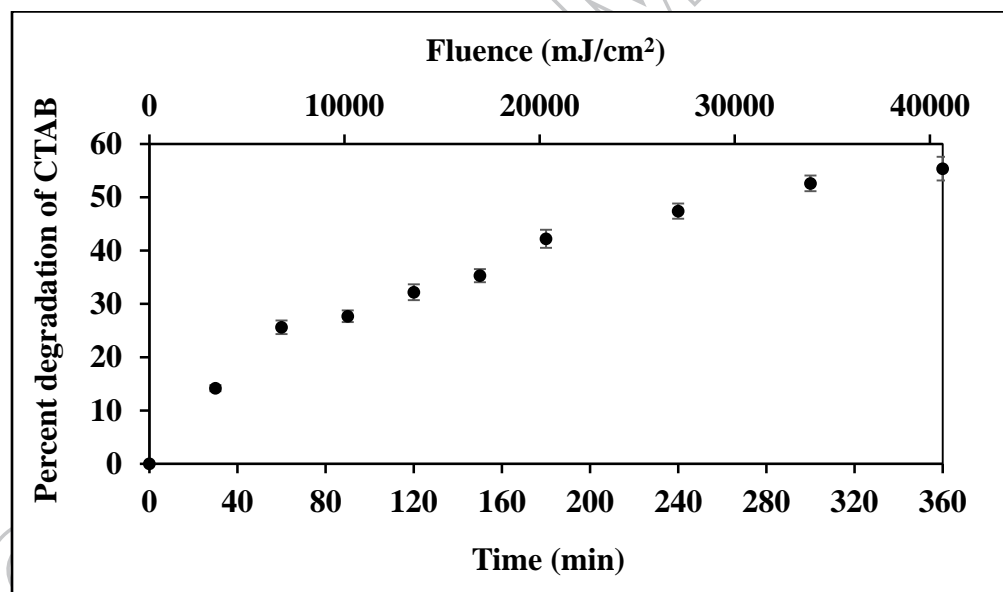


Figure 1

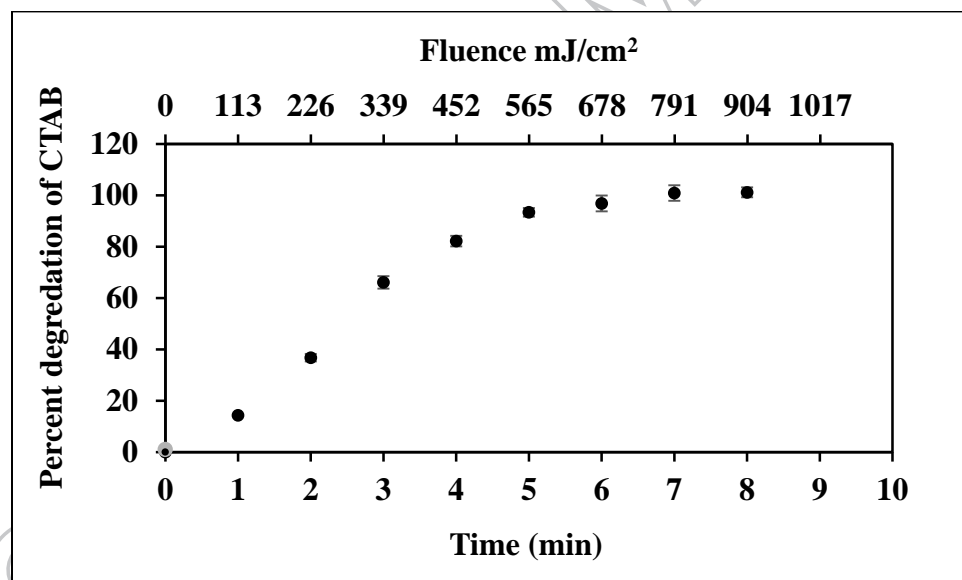


Figure 2

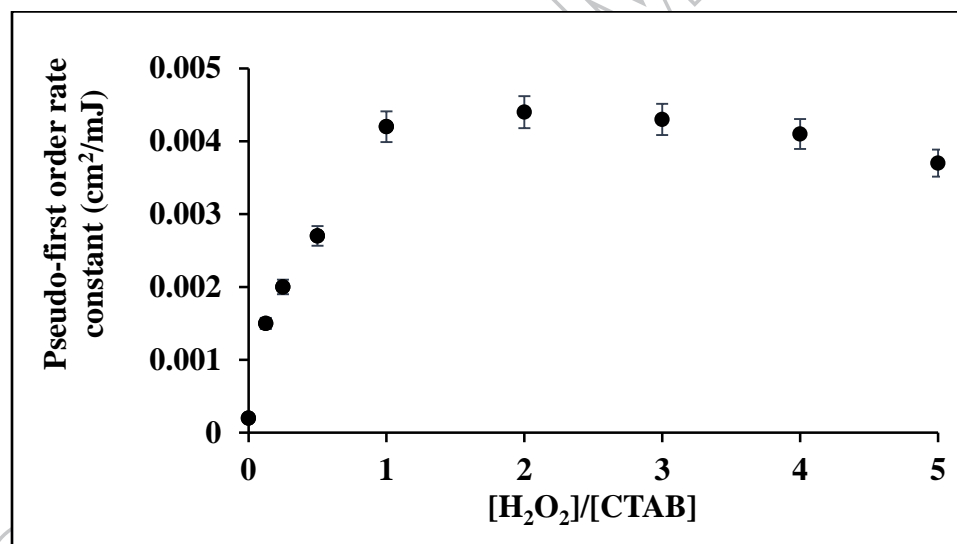


Figure 3



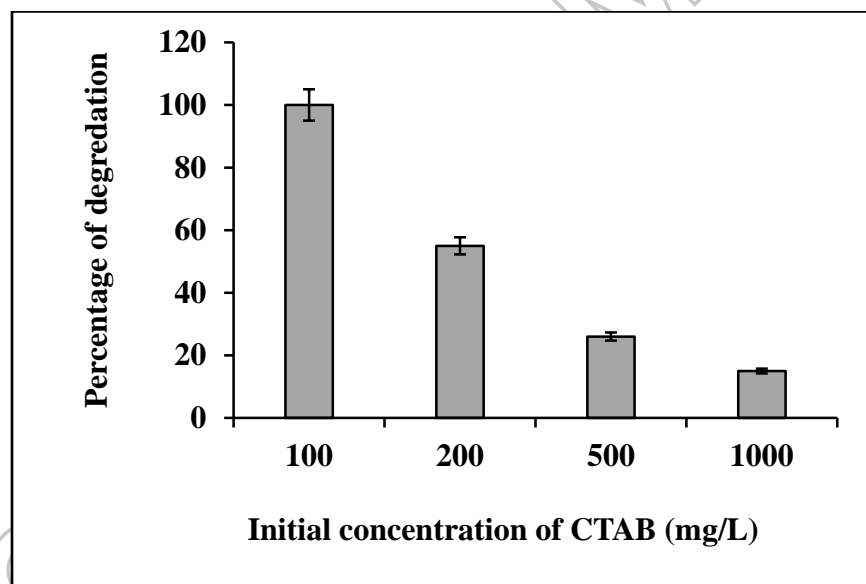


Figure 4

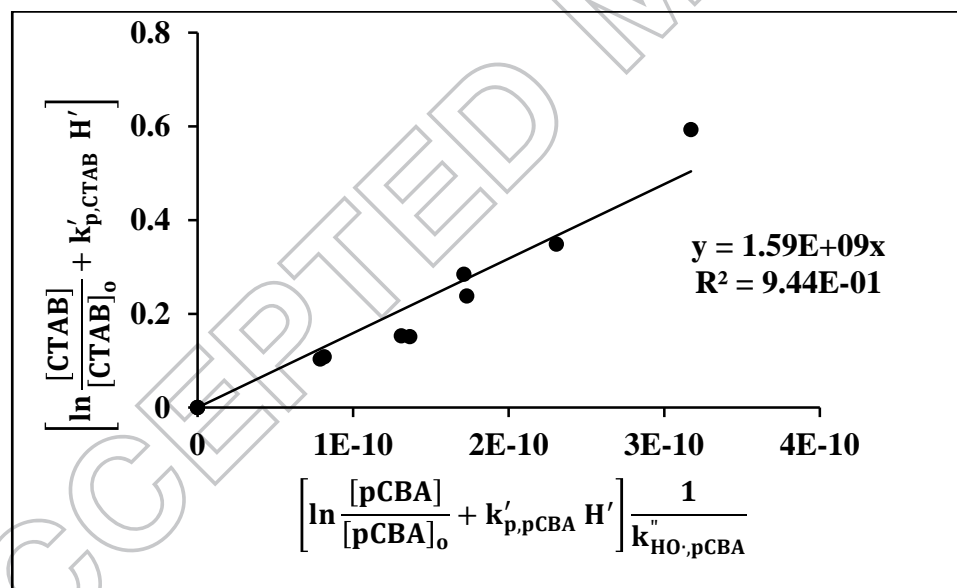


Figure 5

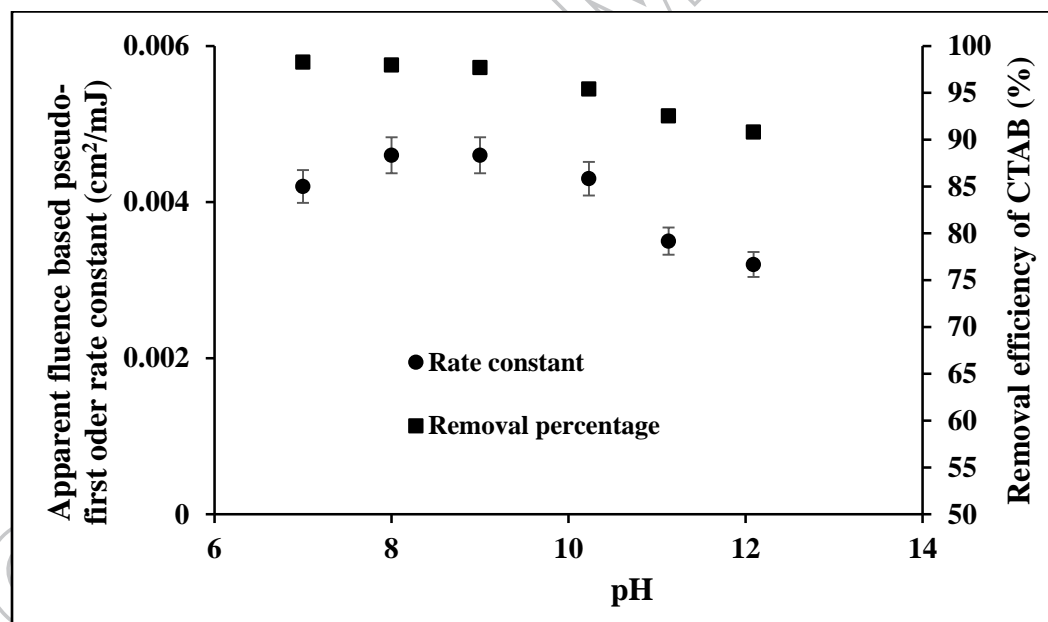


Figure 6

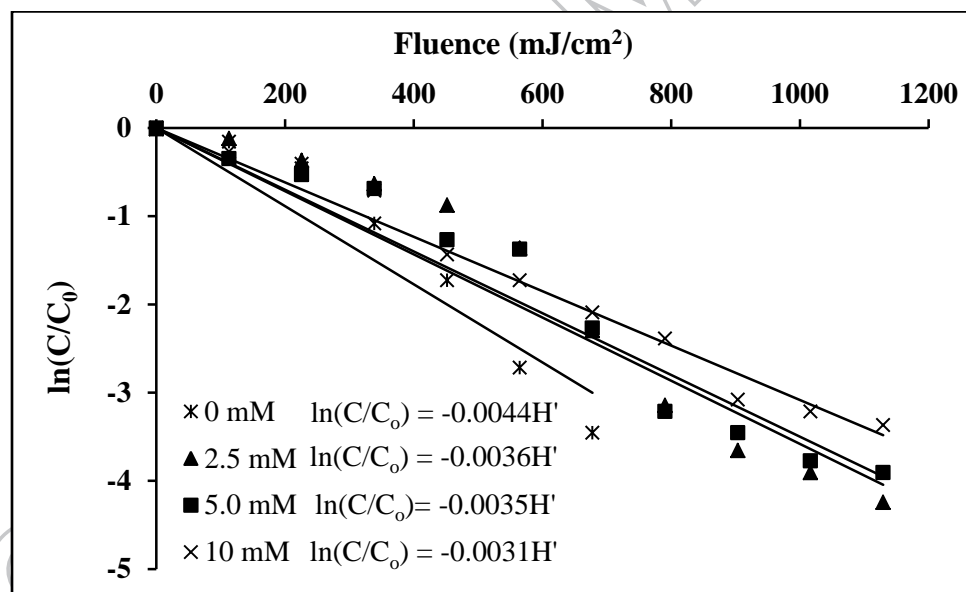


Figure 7

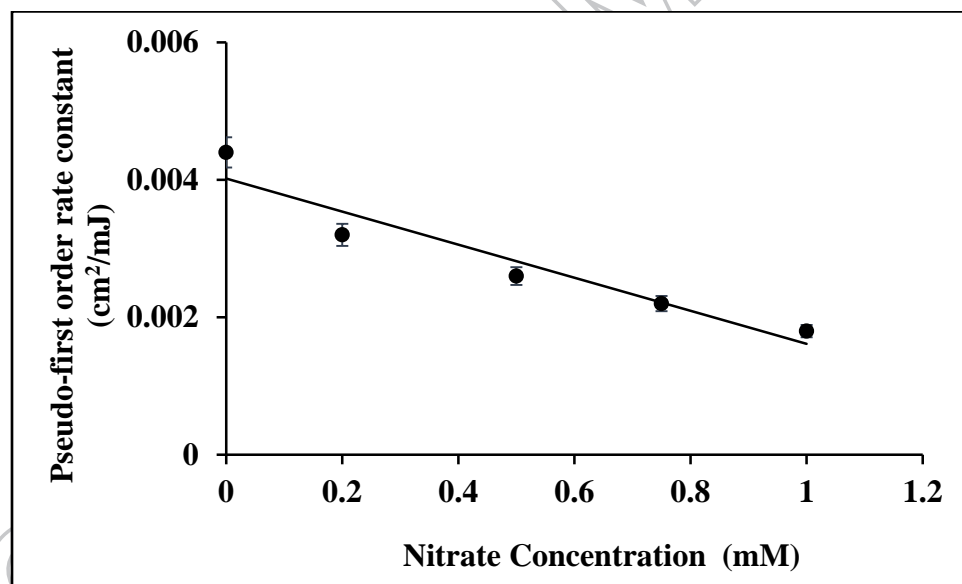


Figure 8

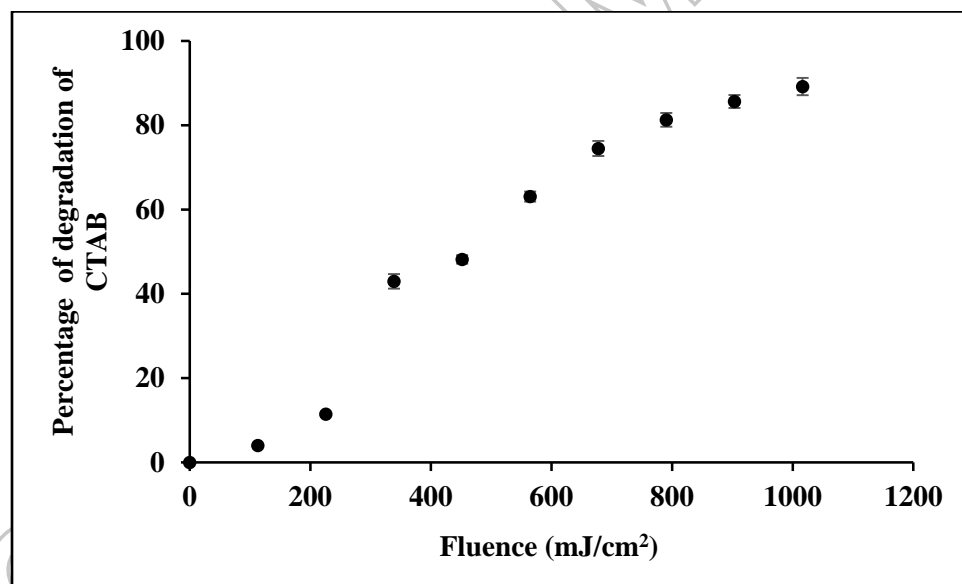


Figure 9

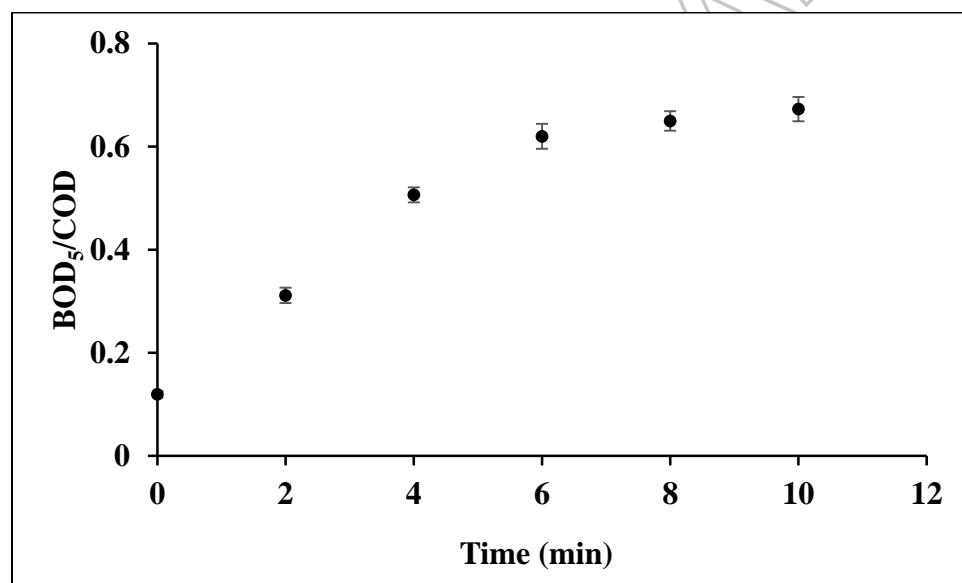


Figure 10